

Design, Synthesis, In Vitro, and In Vivo Characterization of Phenylpiperazines and Pyridinylpiperazines as Potent and Selective Antagonists of the Melanocortin-4 Receptor

Joe A. Tran, Wanlong Jiang, Fabio C. Tucci,[†] Beth A. Fleck, Jenny Wen, Yang Sai, Ajay Madan, Ta Kung Chen, Stacy Markison, Alan C. Foster, Sam R. Hoare, Daniel Marks,[#] John Harman, Caroline W. Chen, Melissa Arellano, Dragan Marinkovic, Haig Bozigian, John Saunders,[‡] and Chen Chen*

Department of Medicinal Chemistry, Department of Pharmacology, Department of Neuroscience and Department of Preclinical Development, Neurocrine Biosciences, Inc., 12790 El Camino Real, San Diego, California 92130

Received September 12, 2007

Benzylamine and pyridinemethylamine derivatives were synthesized and characterized as potent and selective antagonists of the melanocortin-4 receptor (MC4R). These compounds were also profiled in rodents for their pharmacokinetic properties. Two compounds with diversified profiles in chemical structure, pharmacological activities, and pharmacokinetics, **10** and **12b**, showed efficacy in an established murine cachexia model. For example, **12b** had a K_i value of 3.4 nM at MC4R, was more than 200-fold selective over MC3R, and had a good pharmacokinetic profile in mice, including high brain penetration. Moreover, **12b** was able to stimulate food intake in the tumor-bearing mice and reverse their lean body mass loss. Our results provided further evidence that a potent and selective MC4R antagonist with appropriate pharmacokinetic properties might potentially be useful for the treatment of cancer cachexia.

Introduction

Cachexia is a condition characterized by weight loss, wasting of muscle, loss of appetite, and general debility that accompanies many chronic diseases, affects various patient populations, including those with cancer, and is estimated to be responsible for over 20% of all cancer-related deaths.¹ Cancer cachexia significantly impairs quality of life and response to antineoplastic therapies and increases morbidity and mortality of cancer patients. Most current therapeutic strategies to counteract cancer cachexia have proven to be only partially effective.² In the past decade, research into the processes leading to cachexia have provided ideas for more effective therapeutic intervention that have been attempted pharmacologically with encouraging results in animal models and preliminary clinical trials. While recent studies have linked cancer cachexia to endocannabinoid,³ ghrelin,⁴ and other biological systems associated with appetite stimulation and food intake, one key center that is likely involved in the propagation of symptoms of cachexia is the melanocortin system in the hypothalamus and brainstem.⁵

The melanocortin system consists of five cell surface receptors that belong to the class A G-protein-coupled receptor superfamily.⁶ These receptors are activated by the family of melanocyte-stimulating hormone peptide agonists produced from the post-translational processing of pro-opiomelanocortin (POMC^a), including α -, β -, and γ -MSH and adrenocorticotropin hormone (ACTH).⁷ In addition, these receptors are also regulated by the endogenous antagonists agouti-protein and agouti-related protein (AgRP).⁸ The melanocortin-4 receptor (MC4R)^a plays a very important role in

feeding behavior and energy homeostasis in animals and humans.⁹ MC4 receptors are widely expressed in the brain, and MC4R mutations that impair receptor function have been associated with binge eating and obesity in humans.^{10,11} In addition, many studies have demonstrated that MC4R agonists suppress food intake and reduce body weight in animals.¹²

In contrast, recent studies have shown that MC4R antagonists promote food intake and increase weight gain in animals.¹³ Moreover, evidence suggests that cachexia brought about by a variety of illnesses can be attenuated or reversed by blocking MC4R activation within the central nervous system.¹⁴ For example, Wisse and co-workers demonstrate that the peptide MC4R antagonist Ac-Nle(4)-c[Asp(5)-2'-Nal(7)-Lys(10)]- α -MSH(4–10)-NH₂ (SHU9119)¹⁵ reverses body weight loss in mice after intracerebroventricular administration.¹⁶ This effect, however, is diminished in MC4R knock out mice,¹⁷ demonstrating MC4R involvement. Central infusion of AgRP(83–132) also prevents cachexia-related symptoms induced by radiation and colon-26 tumors in mice.¹⁸

While potent peptide antagonists for the MC4 receptor have been known for years, small nonpeptide molecules that antagonize the receptor were only recently discovered.¹⁹ One advantage of nonpeptide molecules is the possibility of delineating pharmacological activity in animals without intracerebroventricular injection if the molecules achieve sufficient brain penetration after peripheral administration. For example, a 2-phenylimidazoline **1** (ML00253764, Figure 1) is a functional MC4R antagonist (IC₅₀ = 103 nM) with poor selectivity versus MC3R, a receptor subtype that is also believed to have a role in feeding regulation²⁰ and has demonstrated efficacy in a cachexia model via subcutaneous administration.^{21,22} Additionally, we have shown that a β -alanine-(2,4-Cl)phenylalanine dipeptide derivative **2** is a potent functional MC4R antagonist with negligible affinity at MC3R.²³ Intraperitoneal administration of **2** effectively stimulates daytime (satiated) food intake and decreases basal metabolic rate in normal animals. Furthermore, this compound attenuates cachexia and preserves lean body mass in a murine cancer model.²⁴ These data provide evidence for

* To whom correspondence should be addressed. Phone: 858-617-7634. Fax: 858-617-7602. E-mail: cchen@neurocrine.com.

[†] Current address: Department of Medicinal Chemistry, Tanabe Research Laboratories, U.S.A., Inc., 4540 Towne Centre Ct., San Diego, CA 92121.

[#] Department of Pediatrics, Oregon Health and Science University, 3181 Southwest Sam Jackson Park Road, Portland, OR 97239.

[‡] Current address: Vertex Pharmaceuticals Inc., 11010 Torreyana Road, San Diego, CA 92121.

^a Abbreviations: MC4R, type 4 melanocortin receptor; MSH, melanocyte-stimulating hormone; AgRP, agouti-related protein; cAMP, cyclic adenosine monophosphate; i.p., intraperitoneal; b/p, brain/plasma.

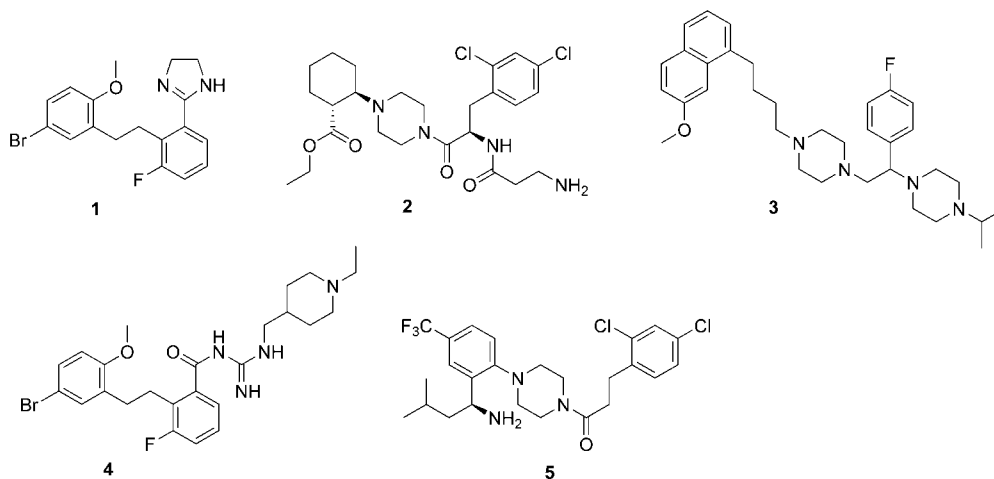


Figure 1. Chemical structures of some small molecule MC4R antagonists.

the potential utility of small molecule MC4R antagonists, particularly in the treatment of cancer cachexia.²⁵

Several MC4R antagonists from different chemical classes have been reported. For example, the structure–activity relationship of bispiperazine derivatives exemplified by **3** has been extensively studied.^{26,27} A series of acylguanidines exemplified by **4** are reported as highly potent MC4R antagonists with brain penetration in rodents.²⁸ Very recently, a series of benzimidazoles are described as potent and selective MC4R antagonists.²⁹ We have previously reported the discovery of a series of piperazinebenzylamines such as **5** ($K_i = 75$ nM) as MC4R antagonists.³⁰ By using **5** as a lead, we started a research effort to improve the MC4R antagonist properties associated with this compound in several categories including potency, metabolism, and pharmacokinetics. Here we report the design, synthesis, and in vitro and in vivo characterization of several compounds based on this initial lead. Among them, *N*-(1*S*-[2-{4-[(2*R*)-methyl-3-(4-chlorophenyl)propionyl]-1-piperazinyl]-5-chlorophenyl]-3-methylbutyl)-3-(dimethylamino)propionamide (**12b**) was identified as potent and selective at the MC4 receptor. It also exhibited suitable pharmacokinetic properties for further evaluation and demonstrated anticachectic activity in a murine cachexia model.

Chemistry

The target benzylamine compounds were synthesized from the protected piperazinebenzylamines **6**,³¹ as shown in Scheme 1. A coupling reaction of the free amine derived from **6a** with 3-(2,4-dichlorophenyl)propionic acid afforded the amides **5** after deprotection with HCl in methanol, which was coupled with *N*-Boc-glycine to give **11** after a TFA treatment.³² Similarly, **6a** was also coupled with 2-methyl-3-(2-methoxy-4-chlorophenyl)propionic acid to provide **7**,³⁰ and compound **8** was obtained from **6b** and 2*R*-methyl-3-(4-chlorophenyl)propionic acid. Reaction of **8** with 3-(*N,N*-dimethylamino)propionic acid under coupling conditions gave the amide **12a**. Compound **12b** was prepared using the same procedure from **6c**. Compound **9** was synthesized from **6d** by the following sequence. A coupling reaction of the free amine of **6d** with *N*-Boc-D-(2,4-Cl)Phe-OH provided an amide that was selectively Boc-deprotected with TFA and reacted with succinaldehydic acid under reductive conditions, followed by a cyclization promoted by EDC under coupling conditions to provide the desired product after deprotection with HCl in methanol.³³ Reductive alkylation of **9** with (2-oxoethyl)carbamic acid *tert*-butyl ester afforded the diamine

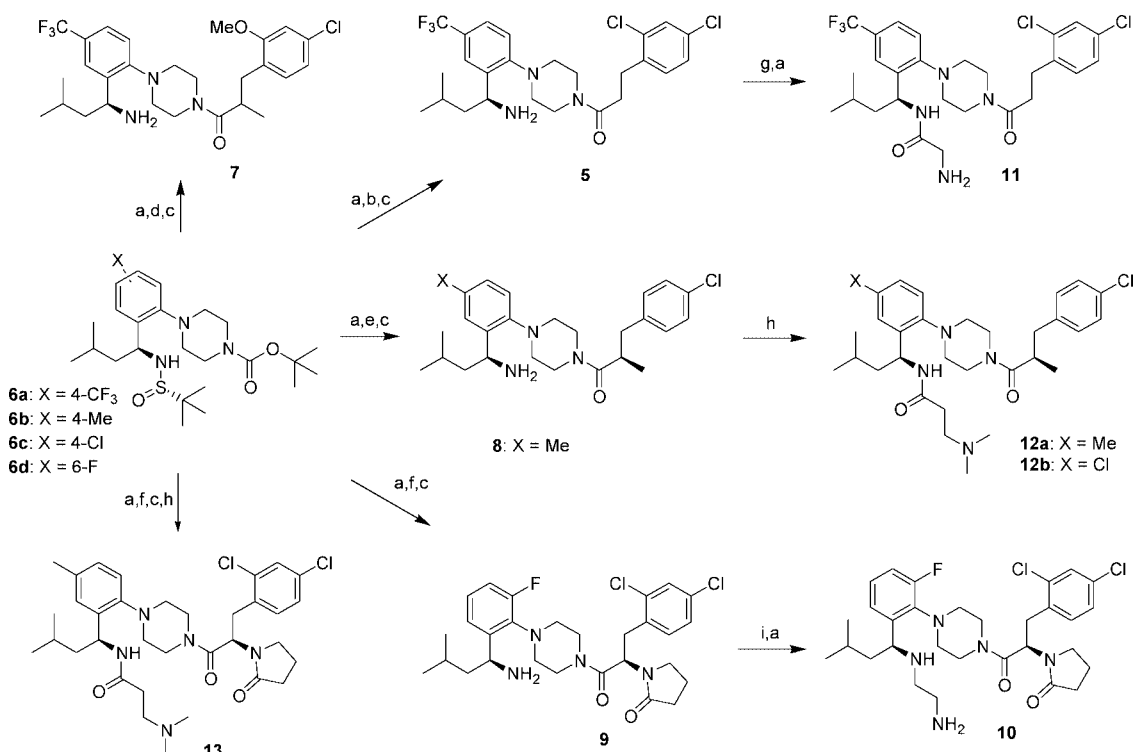
10 after Boc-deprotection.³³ Compound **13** was synthesized from **6b** by a sequence for **9**, followed by a coupling reaction with 3-(dimethylamino)propionic acid.

The optically pure 2*R*-methyl-3-(4-chlorophenyl)propionic acid **16a** and 2*R*-methyl-3-(2,4-dichlorophenyl)propionic acid **16b** were synthesized according to Scheme 2. Stereoselective alkylation of (*S*)-3-propionyl-4-benzylloxazolidine **14** with 4-chlorobenzyl or 2,4-dichlorobenzyl bromide, followed by hydrolysis of the diastereomer **15** promoted by hydrogen peroxide under basic conditions afforded the desired acid **16a** or **16b** in good yield.³⁴

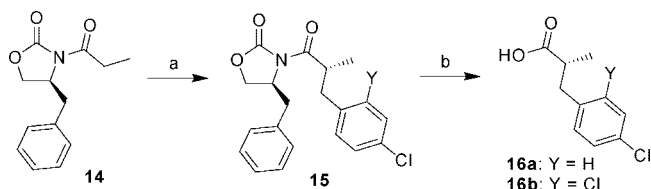
The synthesis of the pyridine derivatives **20–23** is outlined in Scheme 3. 2-Bromo-3-pyridylcarboxaldehyde **17a** was obtained by a formylation of 2-bromopyridine, which was achieved by quenching the carbanion, formed by LDA at -78 °C in THF, with DMF in 19% yield.³⁵ 2-Chloro-6-methyl-3-pyridylcarboxaldehyde **17b** was obtained by the reduction of 2-chloro-3-cyano-6-methylpyridine with Dibal-H in toluene at -10 to 0 °C in 53% yield. These aldehydes were condensed with (*S*)-*tert*-butanesulfinamide to the corresponding pyridylmethylidene sulfinylamides *S*-**18a–b**. Reactions of *S*-**18** with isobutyl lithium afforded the adducts *R*-**19a,b** using conditions similar to those for **6a–d**. Unexpectedly, the stereoselectivity of this reaction was reversed from the benzene analogs **6**, and the major stereoisomer had an *R*-configuration at the newly formed chiral center. The stereochemistry of *R*-**19b** was confirmed by X-ray crystal structure determination (Figure 2). The reason for this reversed stereoselectivity was possibly caused by the participation of the pyridine nitrogen in the chelating process.³¹ The corresponding *S*-**19a** was then synthesized from (*R*)-*tert*-butanesulfinamide using the same procedure. After a TFA treatment of *R*-**19a**, the resultant amine intermediate was coupled with 2,4-dichlorophenylpropionic acid to give *R*-**20a** after an HCl/MeOH treatment. Compound *R*-**20b** was obtained from *R*-**19a** and 2-methyl-3-(2,4-dichlorophenyl)propionic acid. Similarly, a coupling reaction of the free amine derived from *R*-**19b** with (2*R*)-methyl-3-(2,4-dichlorophenyl)propionic acid provided the amide *R*-**21**. Compound *R*-**20b** was further derivatized to *R*-**22** by coupling with glycine, while *R*-**21** was converted to the *N,N*-dimethylpropionamide *R*-**23**. The *S*-isomers, *S*-**20a** and *S*-**22**, were also synthesized from *S*-**19a** for comparison.

Structure–Activity Relationship

The synthesized compounds were tested in a binding assay using membranes from HEK293 cells stably expressing the

Scheme 1^a

^a Reagents and conditions: (a) TFA/CH₂Cl₂, r.t., 1 h; (b) 2,4-ClC₆H₃CH₂CH₂COOH/EDC/HOBt/NaHCO₃/DMF/CH₂Cl₂, r.t., 16 h; (c) HCl/MeOH, r.t., 1 h; (d) 2-MeO-4-Cl-C₆H₃CH₂CHMeCOOH/EDC/HOBt/NaHCO₃/DMF/CH₂Cl₂, r.t., 16 h; (e) *R*-(4-Cl-C₆H₄)CH₂CHMeCOOH/EDC/HOBt/NaHCO₃/DMF/CH₂Cl₂, r.t., 16 h; (f) (i) *N*-Boc-D-(2,4-Cl)Phe-OH/EDC/HOBt/NaHCO₃/DMF/CH₂Cl₂, r.t., 16 h; (ii) TFA/CH₂Cl₂, r.t., 1 h; (iii) OCHCH₂CH₂COOH/NaBH(OAc)₃/HOAc/ClCH₂CH₂Cl, r.t., 24 h; (iv) EDC/HOBt/NaHCO₃/DMF/CH₂Cl₂, r.t., 16 h; (g) *N*-Boc-GlyOH/EDC/HOBt/NaHCO₃/DMF/CH₂Cl₂, r.t., 16 h; (h) Me₂NCH₂CH₂COOH/EDC/HOBt/NaHCO₃/DMF, r.t., 16 h; (i) *N*-Boc-NHCH₂CHO/NaBH(OAc)₃/CH₂Cl₂/r.t. 14 h.

Scheme 2^a

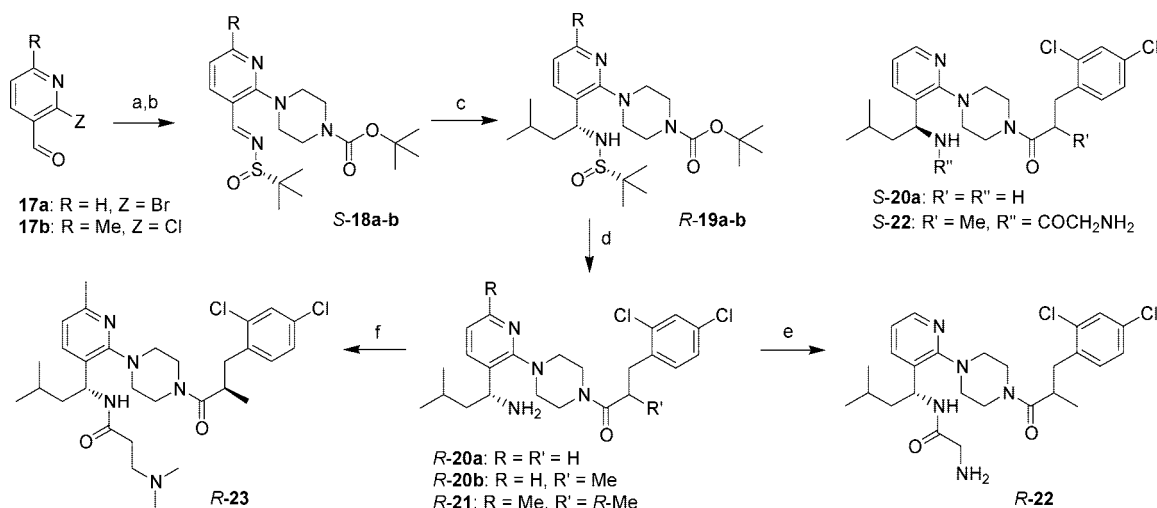
^a Reagents and conditions: (a) NaHMDS/THF, -70°C, 1 h, then 2-*Y*-4-ClC₆H₄CH₂Br, -78 °C to r.t., 6 h; (b) LiOH/H₂O₂/THF/H₂O, 0 °C to r.t., 1.5 h.

human melanocortin-4 receptor as previously described,³⁶ and the results are depicted in Table 1. Compounds **7**, **8**, **10–13** and **R-23** were also tested in a whole cell cAMP assay to study their functional antagonist activity. Selectivity profiles of these compounds at the other melanocortin receptor subtypes were determined in binding assays, and the results are summarized in Table 2.

While the benzylamine **5** displayed a K_i of 75 nM, its glycine derivative **11** (K_i = 19 nM) exhibited increased potency. The 2-methyl-3-(2-methoxy-4-chlorophenyl)propionyl analog **7** (K_i = 14 nM) was over 5-fold better than **5** in binding affinity. Incorporating a *N,N*-dimethylpropionyl group at the benzyl nitrogen of **8** (K_i = 25 nM) improved the potency by about 7-fold (**12a**, K_i = 3.7 nM). Replacing the methyl group of **12a** with a chlorine gave an analog with the similar potency (**12b**, K_i = 3.4 nM). The pyrrolidinone **9** possessed a K_i value of 9.7 nM, which was increased by 10-fold when an aminoethyl group was attached (**10**, K_i = 0.9 nM). In comparison, the *N,N*-dimethylaminopropionamide **13** (K_i = 0.6 nM) also exhibited subnanomolar binding affinity.

For the pyridine compounds **20a**, the *R*-configured compound **R-20a** (K_i = 260 nM) was more potent than its *S*-isomer (**S-20a**, K_i = 890 nM), the opposite of what was seen in the benzylamine series.³⁰ Incorporating a 2-methyl moiety at the 3-(2,4-dichlorophenyl)propionyl group of **R-20a** resulted in a more potent molecule (**R-20b**, K_i = 36 nM). Adding a glycine to **R-20b** improved its potency by 6-fold (**R-22**, K_i = 6 nM), parallel to the result of benzylamines **5** and **11**. Incorporating a methyl group at the 6-position of the pyridine **R-20b** had little effect on its binding affinity (**R-21**, K_i = 44 nM). An almost 20-fold increase in binding affinity from **R-21** was observed for the *N,N*-dimethylaminopropionamide derivative (**R-23**, K_i = 2.5 nM). The potencies of the pyridine derivatives **R-20–23** were quite similar to those of the phenyl analogs (**5** and **7–13**). In the solid state, the piperazine plane was orthogonal to the pyridine ring in 2-piperazinepyridine **R-19b** reflected by its X-ray crystal structure (Figure 2). This conformational feature is also observed for benzene analogs such as Boc-**6a**,³¹ although the overlay of these two X-ray structures indicates that the sulfinylamides point in different directions (Figure 3).

Most of these compounds (**7**, **8**, **10–13** and **R-23**) were very selective at MC4R over the other melanocortin receptor subtypes (Table 2). For example, the pyridine compound **R-23** displayed at least 500-fold selectivity over the other receptor subtypes. The only exception was **7**, which only exhibited 6-fold selectivity at the MC5 receptor compared to MC4R. All of the compounds tested in the functional agonist assay showed no significant stimulation of cAMP accumulation via MC4R at up to 10 μM (data not shown). In the functional antagonist assay, all compounds displayed dose-dependent inhibition of α-MSH-stimulated cAMP accumulation with various potencies (Table 2). The functional IC₅₀ values were typically 20- to 30-fold

Scheme 3^a

^a Reagents and conditions: (a) DMF/DIEA/4-Boc-piperazine, 100 °C, 8 h; (b) *S*-Me₃CSONH₂/Ti(OEt)₄/THF, r.t., 8 h; (c) (i) Me₃Al/THF, -40 °C, 20 min; (ii) *i*-BuLi/THF, -78 °C, 5–8 h; (d) (i) TFA/CH₂Cl₂, r.t., 1 h; (ii) (2,4-Cl₂C₆H₃)CH₂CH(R')COOH/EDC/HOBt/CH₂Cl₂, r.t., 8 h; (e) *N*-Boc-Gly-OH/EDC/HOBt/NaHCO₃/DMF/CH₂Cl₂, r.t., 8 h; (f) Me₂NCH₂CH₂COOH/EDC/HOBt/NaHCO₃/DMF/CH₂Cl₂, r.t., 8 h.

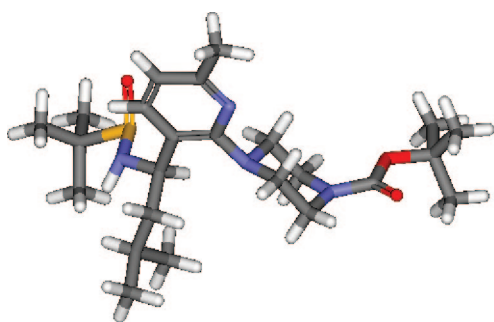


Figure 2. X-ray crystal structure of *R*-19b.

Table 1. Binding Affinity of 5, 7–13, and 20–23 at hMC4R^a

compound	K _i (nM)	compound	K _i (nM)
5	75	13	0.6
7	14	<i>R</i> -20a	260
8	25	<i>S</i> -20a	890
9	9.7	<i>R</i> -20b	36
10	0.9	<i>R</i> -21	44
11	19	<i>R</i> -22	6.0
12a	3.7	<i>S</i> -22	39
12b	3.4	<i>R</i> -23	2.5

^a Data are the average of two or more independent measurements.

higher than the binding affinity *K_i* values, possibly due to the different assay conditions. However, compounds 7, 11, and 12b exhibited a much larger separation between their *K_i* and IC₅₀ values. It is worth noting that these compounds were highly lipophilic, with measured logD values of >3.9 (Table 2).

Pharmacokinetics

Compounds 7, 8, 10, 11, 12b, and *R*-22 were studied in mice for their pharmacokinetic properties (Table 3). After an intravenous (*i.v.*) injection at a 5 mg/kg dose, the benzylamine 7 displayed a high plasma clearance (CL = 62.3 mL/min·kg). Despite its high volume of distribution (*V_d* = 10.3 L/kg), 7 had a short half-life (*t*_{1/2} = 1.9 h), indicative of fast elimination in this species. A concentration of 735 ng/g was detected in the brain at the 1 h time point post-dosing, indicating high brain penetration. A brain/plasma (*b/p*) ratio of 2.3 was calculated at this time point. The absorption of this compound was very fast after a 10 mg/kg oral gavage (*p.o.*), and a maximal concentration

Table 2. Binding Affinity (*K_i*, nM) at the Melanocortin Receptor Subtypes,^a Functional Activity at MC4R and Measured LogD Values of Some MC4R Antagonists

cmpd	binding affinity (<i>K_i</i> , nM)				MC4R function	
	MC1 ^b	MC3	MC4	MC5	IC ₅₀ ^c (nM)	LogD ^d
7	(23%)	320	14	86	1700	4.5
8	3100	1300	25	1000	570	3.0
10	(38%)	750	0.9	850	21	1.8
11	(18%)	1200	19	500	1300	4.5
12a	(34%)	2800	3.7	710	160	2.4
12b	(20%)	710	3.4	600	930	3.9
13	8400	820	0.6	520	19	3.9
<i>R</i> -23	6400	3300	2.5	1200	49	3.3

^a Data are the average of two or more independent measurements. ^b The percentage inhibition at 10 μM concentration is indicated in parenthesis. ^c Dose-dependent inhibition of α-MSH-stimulated cAMP production via MC4R. ^d The logD value was measured using a shake-flake method.

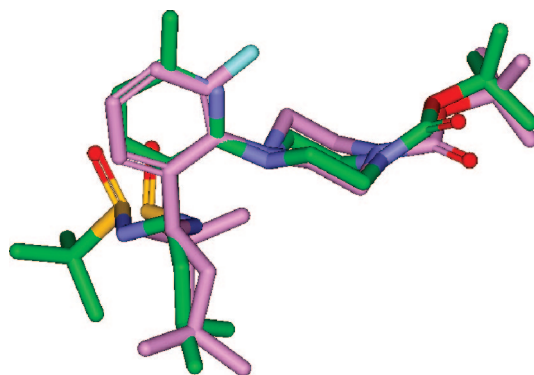


Figure 3. Overlay of pyridylpiperazine *R*-19 and phenylpiperazine 6a.

(*C*_{max} = 99 ng/mL) appeared at 0.25 h (*T*_{max}), resulting in an area under curve (AUC) of 249 ng/mL·h and a low oral bioavailability (*F*% = 8.6). In comparison, the benzylamine 8 had a moderate plasma clearance (CL = 33.3 mL/min·kg) and a high *V_d* value of 10.2 L/kg, resulting in a *t*_{1/2} of 3.5 h. The lipophilicity of 8 (LogD = 3.0) was significantly lower than that of 7 (LogD = 4.5), which might contribute to its lower plasma clearance. The brain penetration of 8 was high (*b/p* = 2.9 and 1.4 at 1 h and 4 h, respectively) and its oral bioavailability increased to 34% compared to 7. The less

Table 3. Pharmacokinetic Profiles of MC4R Antagonists in CD-1 Mice^a

compd	CL (mL/min·kg)	V _d (L/kg)	t _{1/2} (h)	C _b (ng/g) at 1, 4 h	b/p ratio at 1, 4 h	T _{max} (h)	C _{max} (ng/mL)	oral AUC (ng/mL·h)	F (%)
7	62.3	10.3	1.9	735, 122	2.3, 1.9	0.25	99	249	8.6
8	33.3	10.2	3.5	940, 330	2.9, 1.4	0.5	267	1762	34.4
10	15	13	10	63, 53	0.14, 0.23	2.0	552	1950	19.5
11	26.9	8.8	3.8	43, 33	0.08, 0.17	2.0	115	687	11.2
12b	36	11	3.5	800, 177	2.4, 2.2	0.5	132	1160	23.0
R-22	37.4	16.8	5.2	35, 14	0.07, 0.15	0.5	288	551	12.6

^a Three animals were dosed intravenously at 5 mg/kg and orally at 10 mg/kg; brain concentrations were taken from the i.v. dosing.

Table 4. Pharmacokinetic Profiles of **12a,b**, **13**, and **R-23** in Sprague–Dawley Rats^a

compd	CL (mL/min·kg)	V _d (L/kg)	t _{1/2} (h)	T _{max} (h)	C _{max} (ng/mL)	oral AUC (ng/mL·h)	F(%)	C _b (ng/g) at 1, 4 h	b/p ratio at 1, 4 h
12a	15.0	4.1	3.1	5.3	196	2358	19	12, 36	0.2, 0.3
12b	13.0	2.5	2.2	6.0	163	1867	18	3, 27	0.1, 0.3
13	38.7	8.8	2.6	4.0	40	393	8.7	1.5, 15	0.2, 0.3
R-23^b	64.9	18.6	3.3	2.0	60	517	19.6	15, 29	0.2, 0.2

^a Three animals were dosed intravenously at 5 mg/kg and orally at 10 mg/kg; brain concentrations were taken from p.o. dosing. ^b i.v. dose at 2.5 mg/kg.

lipophilic diamine **10** (logD = 1.8) had a low plasma clearance despite its high tissue distribution (V_d = 13 L/kg), resulting in a very long t_{1/2} of 10 h in mice. However, this compound had low brain penetration, with a b/p ratio of 0.14–0.23. In an in vitro Caco-2 assay, **10** exhibited a P_{app} of 20 nm/s from apical to basolateral direction, which was not significantly different from that of compound **8** (P_{app} = 18 nm/s). Its permeation from the basolateral to apical direction was about 3.4-fold higher than the apical to basolateral direction (ba/ab ratio = 3.4), suggesting a possible efflux mechanism involving P-glycoprotein.³⁷ However, this value was also similar to that of **8** (ba/ab ratio = 4.4), indicating that the P-glycoprotein transporter might not be the only determinant for the difference between these two compounds in brain penetration. The plasma exposure of **10** after oral dosing was high (AUC = 1950 ng/mL·h), and the absolute bioavailability was about 20%.

The aminoacetamide **11** had a moderate plasma clearance, but its brain penetration was low, similar to **10**. This phenomenon might be associated with the high polar surface area of these two compounds (PSA = 79 and 82 Å² for **11** and **10**, respectively). The *N,N*-dimethylpropionamide **12b** displayed a moderate clearance and a t_{1/2} of 3.5 h. Its brain penetration was much better (b/p ratio = 2.2–2.4, PSA = 56 Å²) than the diamine **10** and the aminoacetamide **11**. The oral absorption of **12b** was fast (T_{max} = 0.5 h) and the oral bioavailability was 23% in this species. The pyridine **R-22** was also profiled in this study, and its PK parameters were not significantly different from that of its close phenyl analog **11**, except for a higher V_d value, which resulted in a longer t_{1/2}.

Because the *N,N*-dimethylpropionamide **12b** exhibited a desirable PK profile in mice (high brain penetration, good oral bioavailability, and moderate t_{1/2}), this compound and its close analogs **12a**, **13**, and **R-23** were also profiled in rats for their pharmacokinetic properties (Table 4). Compounds **12a** and **12b** displayed very similar profiles in rats. The volume of distribution of **12b** (V_d = 2.5 L/kg) was much lower than that in mice, which resulted in a shorter t_{1/2} (2.2 h). Absorption was slow and the C_{max} appeared at 6 h after oral dosing. The whole brain concentration of **12b** in rats was much lower than that in mice, and the b/p ratio was observed to be 0.1 and 0.3, respectively, at the 1 and 4 h time points after an oral administration. Compound **13**, which had a similar lipophilic profile to **12b**, displayed a large V_d in this species. However, its t_{1/2} was not much longer than that of **12b** due to the high plasma clearance. The pyridine compound **R-23** had a very large V_d of 18.6 L/kg, which might be associated with its moderate basicity of the 2-aminopyridine structure (calculated pK_a = 9.3 for piperazinepyridine), although its measured lipophilicity at pH 7.4

Table 5. Pharmacokinetic Properties of **12b** in Dogs and Monkeys^a

species	dog	monkey
i.v. dose (mg/kg)	5	5
CL (mL/min·kg)	29.4	24.3
V _d (L/kg)	11.8	8.5
t _{1/2} (h)	4.7	4.1
AUC (ng/mL·h)	2509	3700
p.o. dose (mg/kg)	10	10
C _{max} (ng/mL)	142	108
T _{max} (h)	1.0	2.7
AUC (ng/mL·h)	1475	1070
F (%)	29.4	13.1

^a Data are the average of three animals.

(logD = 3.3) was only slightly lower than its close phenyl analog **12b** (logD = 3.9). The plasma clearance of **R-23** was high (CL = 64.9 mL/min·kg), which resulted in a moderate t_{1/2} of 3.3 h. Its plasma exposure and brain concentration after oral dosing was low. Overall, this pyridine compound did not show a better PK profile than its phenyl analogs such as **12b**.

The pharmacokinetic properties of **12b** were also profiled in monkeys and dogs (Table 5). The volume of distribution of **12b** was high in both dogs (V_d = 11.8 L/kg) and monkeys (V_d = 8.5 L/kg), which matched that in mice (V_d = 11 L/kg), but not in rats (V_d = 2.5 L/kg). The low V_d value in rats may be associated with a species-specific phenomenon (e.g., high plasma protein binding). The half-life (4.7 and 4.1 h, respectively, for dogs and monkeys) was moderate and the oral bioavailability was good in dogs, but lower in monkeys.

In Vivo Efficacy in Mouse Cachexia Model

Previously we have shown that when administered twice daily (3 mg/kg s.c.) for 4 days to C57BL/6, mice bearing subcutaneous Lewis lung carcinoma tumors, **10**, stimulated food intake by 82% relative to vehicle-treated controls. The lean body mass of the tumor-bearing mice treated with **10** (−0.5%) significantly increased (9%) over that of tumor-vehicle treated animals (−9.5%), demonstrating a positive effect in this cachexia model.³⁸

For the current in vivo study, C57BL/6J male mice were inoculated with Lewis lung carcinoma (LLC) tumor cells. Beginning 11 days after LLC inoculation, animals were treated over 4 days with **12b** twice daily (3 and 9 mg/kg, i.p.). LLC tumor bearing mice treated with a high dose of **12b** showed a significant increase in food intake relative to vehicle-treated tumor bearing controls (Figure 4A). Body weight was also significantly increased in mice treated with **12b** in both dose groups. Analysis of body composition with dual-energy X-ray absorptometry (DEXA) demonstrated that the greater increase

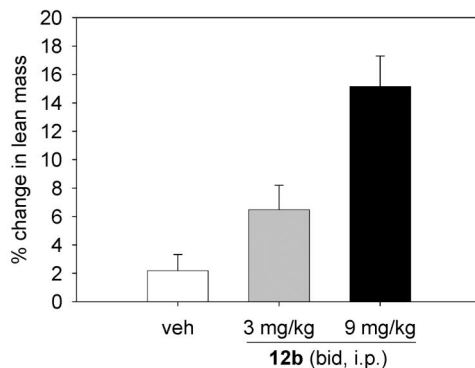
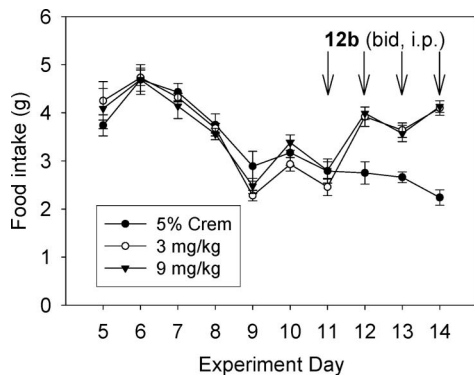


Figure 4. The effects of compound **12b** (i.p., 3 and 9 mg/kg twice per day) on food intake (4A, left) and lean body mass (4B, right) in tumor-bearing mice.

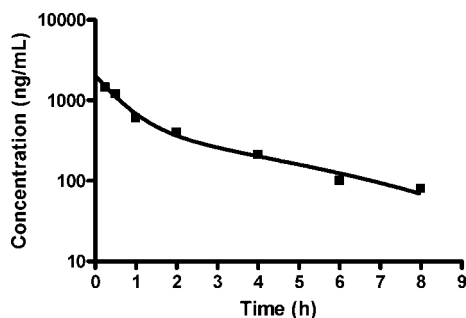


Figure 5. Time–concentration curve of **12b** after an i.p. administration (10 mg/kg) to CD-1 mice ($n = 3$; $C_{\max} = 1521$ ng/mL; $T_{\max} = 0.3$ h; $AUC = 3073$ ng/mL·h).

of body weight in **12b**-treated mice was due to sparing of lean body mass (Figure 4B). Tumor bearing animals treated with vehicle demonstrated an ~2% increase in lean body mass (LBM) over the course of the 14 day experiment, whereas tumor-bearing animals treated with **12b** increased their LBM by ~7% for the 3 mg/kg group and ~15% for the 9 mg/kg group, demonstrating a dose–response effect.

Pharmacokinetic and Pharmacodynamic Relationship

The binding affinity (K_i) of **12b** at the mouse melanocortin-4 receptor was determined to be 18 nM, which was much lower than that of **10** ($K_i = 0.71$ nM at mouse MC4R). It also bound to the mouse melanocortin-3 receptor with a moderate affinity ($K_i = 340$ nM). We profiled the pharmacokinetics of **12b** in CD-1 mice via an intraperitoneal (i.p.) administration of a 10 mg/kg dose. Compound **12b** reached a maximal plasma concentration (C_{\max}) of 1521 ng/mL (~2.7 μ M, Figure 5). At 8 h post-dosing, the plasma concentration was about 100 ng/mL (~0.18 μ M). Therefore, although the free fraction of the compound in the brain was unknown, the total brain concentration of **12b** at any time point during the in vivo efficacy study should have been 5-fold above its K_i value (18 nM) for a twice a day administration at a 3 mg/kg dose, considering its high brain/plasma ratio of ~2 and assuming linear pharmacokinetics.

Because ghrelin agonists have demonstrated efficacy in cachexia models,³⁹ we also measured these MC4 antagonists against the ghrelin receptor in vitro. Compound **10** was a moderately potent full agonist of the ghrelin receptor, with an EC_{50} value of 79 nM (107% intrinsic activity). In comparison, **12b** was a much weaker partial agonist with an EC_{50} of 720 nM and IA of 47% at the ghrelin receptor.

Both **10** and **12b** exhibited low binding affinity at the ghrelin receptor. Compound **10** had 100-fold selectivity for the mouse

MC4R over the ghrelin receptor (K_i of 0.7 nM and 720 nM, respectively) and **12b** had a K_i value of 460 on the ghrelin receptor. The extent to which the ghrelin component of these compounds contributes to the efficacy in the mouse cachexia model is unclear, but unlikely to be significant, especially for compound **12b** due to its low intrinsic activity.

Metabolic Profile of **12b**

Compound **12b** was a fairly lipophilic molecule with a logD value of 3.9, measured by a shake-flask method. It did not show significant inhibitory activity at the major liver enzymes CYP1A2, CYP3A4, CYP2D6, CYP2C9, and CYP2C19 ($IC_{50} > 10$ μ M). In liver microsomes of various species, **12b** showed moderate metabolic stability and the scaled systemic clearances were 57, 35, 38.1, 17.1, and 18.5 mL/min·kg, respectively, in mouse, rat, monkey, dog, and human. After incubation with human liver microsomes, two major metabolites were observed. The metabolic profiles were similar in liver microsomes of CD-1 mice, Sprague–Dawley rats, rhesus monkeys, and beagle dogs. One of the major metabolites was identified as the *N*-demethylation product. The other was characterized as the hydroxylation of the piperazine ring based on MS-MS analyses.

Conclusion

In conclusion, a series of α -isobutylbenzylamine derivatives **7–13** were synthesized and studied as potent and selective antagonists of the melanocortin-4 receptor. Pyridine alternatives **20–23** were also studied to compare to their benzene analogs. Although potent and selective MC4R antagonists such as **R-23** were identified, and these pyridine derivatives did not exhibit an advantage in pharmacokinetic properties over their phenyl analogs. Compounds **10** and **12b** were tested in a murine cachexia model and efficacy was demonstrated. Our results provide more evidence that a potent and selective MC4R antagonist has a potential utility in the treatment of cancer cachexia.

Experimental Section

Chemistry. General Methods. NMR spectra were recorded on a Varian 300 MHz spectrometer with TMS as an internal standard. ¹³C NMR spectra were recorded at 75 MHz. Chemical shifts are reported in parts per million (δ), and signals are expressed as s (singlet), d (doublet), t (triplet), q (quartet), m (multiplet), or br (broad). High resolution mass spectra were measured at the Scripps Center for Mass Spectrometry using MALDI-FTMS. Purity measurements were performed on an HP Agilent 1100 HPLC-MS (detection at 220 and 254 nm).

(1S)-[2-{4-[3-(2,4-Dichlorophenyl)propionyl]-1-piperazinyl]-5-(trifluoromethyl)phenyl]-3-methylbutylamine Trifluoroacetate (**5**).

Trifluoroacetic acid (0.2 mL) was added to a solution of 4-[2-[(1*S*)-((*S*)-*tert*-butanesulfinylamino)-3-methylbutyl]-4-(trifluoromethyl)phenyl]-1-piperazinecarboxylic acid *tert*-butyl ester (**6a**, 50 mg, 0.096 mmol) in dichloromethane (0.8 mL), and the mixture was stirred at r.t. for 50 min. The reaction mixture was basified with saturated aqueous NaHCO₃ solution (5 mL) and extracted with EtOAc (30 mL). The organic layer was dried over Na₂SO₄ and concentrated in vacuo to provide 4-[2-[(1*S*)-((*S*)-*tert*-butanesulfinylamino)-3-methylbutyl]-4-(trifluoromethyl)phenyl]-1-piperazine as white foam, which was dissolved in DMF/dichloromethane (1:3, 1 mL). NaHCO₃ (16.2 mg, 0.192 mmol), 3-(2,4-dichlorophenyl)propionic acid (25.3 mg, 0.12 mmol), HOBt (15.5 mg, 0.12 mmol), and EDC (22.0 mg, 0.12 mmol) were sequentially added to this solution. The reaction mixture was stirred at r.t. overnight, diluted with EtOAc (20 mL), washed with 5% aqueous HCl (5 mL), saturated aqueous NaHCO₃ (5 mL), and brine (5 mL), and dried over Na₂SO₄. The solution was concentrated in vacuo to provide a crude product that was dissolved in MeOH (2 mL) and treated with HCl (58 μ L 4 N HCl in dioxane). The mixture was stirred at r.t. for 1 h and concentrated in vacuo. The residue was purified by flash column chromatography (5~15% MeOH in dichloromethane) to provide the titled compound **5** as a yellowish foam (55.2 mg, 93%). HPLC purity: 100% (220 and 254 nm); ¹H NMR (CD₃OD, TFA salt): 0.96 (d, *J* = 6.6 Hz, 3H), 1.04 (d, *J* = 6.6 Hz, 3H), 1.38–1.52 (m, 1H), 1.68–1.80 (m, 1H), 1.80–1.92 (m, 1H), 2.77 (t, *J* = 7.5 Hz, 2H), 2.82–3.12 (m, 5H), 3.21–3.27 (m, 2H), 3.50–3.80 (m, 3H), 5.00–5.08 (m, 1H), 7.22–7.38 (m, 3H), 7.46 (d, *J* = 1.8 Hz, 1H), 7.73 (dd, *J* = 1.8, 8.3 Hz, 1H), 7.83 (d, *J* = 1.8 Hz, 1H). MS: 516 (MH⁺).

***N*-(1*S*)-[2-[4-[3-(4-Chlorophenyl)propionyl]-1-piperazinyl]-5-(trifluoromethyl)phenyl]-3-methylbutylamine (11).** In a 4 dram vial, the crude (1*S*)-[2-[4-[3-(2,4-dichlorophenyl)propionyl]-1-piperazinyl]-5-(trifluoromethyl)phenyl]-3-methylbutylamine (**5**, 0.70 g), *N*-Boc-glycine (0.19 g, 1.35 mmol), NaHCO₃ (208 mg, 2.48 mmol), and HOBt (0.183 g, 1.35 mmol) were combined and dissolved in dichloromethane (3 mL). The mixture was capped and stirred at r.t. for 15 min. EDC (0.258 g, 1.35 mmol) was added, and the mixture was stirred for 1 h. The mixture was diluted with dichloromethane (2 mL) and washed with saturated aqueous NaHCO₃ (2 \times 1 mL) and brine (1 mL). The organic layer was dried over anhydrous Na₂SO₄, filtered, and concentrated by a stream of nitrogen. The residue was dissolved in (1:1) TFA/CH₂Cl₂, and the solution was stirred at r.t. for 30 min. The mixture was concentrated in vacuo, and the residue was purified by column chromatography on silica using 1:1 hexane/ethyl acetate as the eluent to afford the titled compound as a light yellow solid (55 mg, 70% yield). HPLC purity: 98% (220 nm) and 97% (254 nm). ¹H NMR (CD₃OD, TFA salt): 0.97 (d, *J* = 6.2 Hz, 3H), 0.97 (d, *J* = 6.2 Hz, 3H), 1.22–1.35 (m, 1H), 1.37–1.50 (m, 1H), 1.52–1.68 (m, 1H), 2.56–2.70 (m, 2H), 2.77 (t, *J* = 7.5 Hz, 2H), 3.07 (t, *J* = 7.5 Hz, 2H), 3.15–3.27 (m, 2H), 3.50–3.90 (m, 6H), 5.65–5.72 (m, 1H), 7.24–7.38 (m, 3H), 7.46 (d, *J* = 2.2 Hz, 1H), 7.53 (dd, *J* = 1.8, 8.3 Hz, 1H), 7.60 (d, *J* = 1.8 Hz, 1H). MS: 573 (MH⁺). HRMS (MH⁺) calcd for C₂₇H₃₄Cl₂F₃N₄O₂, 573.2011; found, 573.2009.

(1*S*)-[2-[4-[2-Methyl-3-(2-methoxy-4-chlorophenyl)propionyl]-1-piperazinyl]-5-(trifluoromethyl)phenyl]-3-methylbutylamine Mesylate (7**).** This compound was prepared using a procedure similar to that for **5** from **6a** and 2-methyl-3-(2-methoxy-4-chlorophenyl)propionic acid. White powder; HPLC purity: 100% (220 and 254 nm). ¹H NMR (DMSO-*d*₆): 0.85 (d, *J* = 6.6 Hz, 3H), 0.92 (d, *J* = 6.3 Hz, 3H), 0.99 and 1.00 (d, *J* = 6.6 Hz, 3H), 1.38 (m, 1H), 1.53 (m, 1H), 1.76 (m, 1H), 2.29 (s, 3H, MeOH), 2.30–3.20 (m, 3H), 3.30–3.70 (m, 8H), 3.80 and 3.83 (s, 3H), 4.79 (m, 1H), 6.92–7.12 (m, 3H), 7.35 (t, *J* = 8.7 Hz, 1H), 7.72 (d, *J* = 8.1 Hz, 1H), 7.93 (s, 1H), 8.20 (brs, 3H). MS: 526 (MH⁺). Anal. (C₂₇H₃₅ClF₃N₃O₂·MeSO₃H·2H₂O) C, H, N.

(1*S*)-[2-[4-[(2*R*)-Methyl-3-(4-chlorophenyl)propionyl]-1-piperazinyl]-5-methylphenyl]-3-methylbutylamine Mesylate (8**).** This compound was prepared using a procedure similar to that for **5** from **6b** and 2*R*-methyl-3-(4-chlorophenyl)propionic acid (**16a**). White powder; HPLC purity: 97.9% (220 nm) and 97.7% (254 nm).

¹H NMR (DMSO-*d*₆, free base): 0.84 (d, *J* = 6.0 Hz, 3H), 0.89 (d, *J* = 6.0 Hz, 3H), 1.04 (d, *J* = 6.6 Hz, 3H), 1.43 (m, 1H), 1.58 (m, 1H), 2.26 (s, 3H), 2.45 (m, 1H), 2.62 (dd, *J* = 5.7, 12.6 Hz, 1H), 2.80 (m, 3H), 2.90–3.50 (m, 8H), 4.56 (t, *J* = 6.9 Hz, 1H), 6.40 (brs, 1H), 6.94 (brs, 1H), 7.07 (d, *J* = 8.1 Hz, 1H), 7.24 (d, *J* = 8.1 Hz, 2H), 7.30 (s, 1H), 7.36 (d, *J* = 8.1 Hz, 2H). MS: 442 (MH⁺). Anal. (C₂₆H₃₆ClN₃O·1.3MeSO₃H·2.5H₂O) C, H, N, S.

(1*S*)-[2-[4-[(2*R*)-(2-Oxo-1-pyrrolidinyl)-3-(2,4-dichlorophenyl)propionyl]-1-piperazinyl]-3-fluorophenyl]-3-methylbutylamine (9**).** TFA (4.5 mL) was added to a solution of 4-[2-[(1*S*)-((*S*)-*tert*-butanesulfinylamino)-3-methylbutyl]-6-fluorophenyl]-1-piperazinecarboxylic acid *tert*-butyl ester (**6d**, 1.02 g, 2.17 mmol) in dichloromethane (18 mL), and the mixture was stirred at r.t. for 45 min. The reaction mixture was basified with saturated aqueous NaHCO₃ solution (100 mL) and extracted with EtOAc (2 \times 100 mL). The organic layer was dried over Na₂SO₄ and concentrated in vacuo to provide 4-[6-fluoro-2-[(1*S*)-((*S*)-*tert*-butylsulfinylamino)-3-methylbutyl]phenyl]-1-piperazine as white foam, which was dissolved in DMF/CH₂Cl₂ (1:3, 12 mL). NaHCO₃ (0.365 g, 4.34 mmol), *N*-Boc-D-(2,4-Cl)Phe-OH (0.871 g, 2.61 mmol), HOBt (0.352 g, 2.61 mmol), and EDC (0.50 g, 2.61 mmol) were sequentially added to this solution. The reaction mixture was stirred at r.t. overnight. The mixture was diluted with EtOAc (60 mL), washed with 5% aqueous HCl (15 mL), saturated aqueous NaHCO₃ (15 mL) and brine (15 mL), and was dried over Na₂SO₄. The solution was concentrated in vacuo, and the residue was purified by flash column chromatography (30~60% EtOAc in hexanes) to provide *N*-[(1*S*)-[2-[4-[(2*R*)-(*tert*-butoxycarbonylamino)-3-(2,4-dichlorophenyl)propionyl]-1-piperazinyl]-3-fluorophenyl]-3-methylbutyl]-(*S*)-*tert*-butanesulfinamide as a white solid (1.295 g, 87%).

TFA (1 mL) was added to a solution of the above compound (338 mg, 0.494 mmol) in dichloromethane (4 mL), and the mixture was stirred at r.t. for 1 h. The reaction mixture was basified with saturated aqueous NaHCO₃ solution (30 mL) and extracted with EtOAc (2 \times 30 mL). The organic layer was dried over Na₂SO₄ and concentrated in vacuo to provide *N*-[(1*S*)-[2-[4-[(2*R*)-amino-3-(2,4-dichlorophenyl)propionyl]-1-piperazinyl]-3-fluorophenyl]-3-methylbutyl]-(*S*)-*tert*-butanesulfinamide as a white foam, which was dissolved in 1,2-dichloroethane (5 mL). This solution was treated with acetic acid (118 μ L, 1.98 mmol) and succinic semialdehyde (374 μ L 15 wt% solution in water, 0.592 mmol) and stirred for 30 min NaBH(OAc)₃ (220 mg, 0.987 mmol) was added, and the mixture was stirred at r.t. for 24 h. LC-MS showed the reductive amination was completed and the ratio of lactam product (M.W. = 653) to carboxylic acid product (M.W. = 671) was 1:1. The reaction was quenched with brine (10 mL), and the products were extracted with EtOAc (40 mL), dried over Na₂SO₄, filtered, and concentrated in vacuo. The residue was dissolved in DMF/CH₂Cl₂ (1:3, 10 mL), and NaHCO₃ (0.083 g, 0.988 mmol), HOBt (0.080 g, 0.592 mmol), and EDC (0.113 g, 0.592 mmol) were sequentially added. The reaction mixture was stirred at r.t. overnight, diluted with EtOAc (60 mL), washed with 5% aqueous HCl (10 mL), saturated aqueous NaHCO₃ solution (10 mL), and brine (10 mL), and dried over Na₂SO₄. After filtration, the solution was concentrated in vacuo, and the residue was purified by flash column chromatography (40~70% EtOAc in hexanes) to provide *N*-[(1*S*)-[2-[4-[(2*R*)-(2-oxo-1-pyrrolidinyl)-3-(2,4-dichlorophenyl)propionyl]-1-piperazinyl]-3-fluorophenyl]-3-methylbutyl]-(*S*)-*tert*-butanesulfinamide as a white solid (0.239 g, 74%).

To a solution of the above compound (239 mg, 0.366 mmol) in MeOH (4 mL) was added 2 equiv HCl (183 μ L, 4 N HCl in dioxane), and the mixture was stirred at r.t. for 30 min. The mixture was concentrated in vacuo to give the crude product. A small sample was purified using HPLC-MS. Light yellow foam; HPLC purity: 100% (220 nm). ¹H NMR (CD₃OD, free base): 0.91 (d, *J* = 6.2 Hz, 3H), 0.95 (d, *J* = 6.2 Hz, 3H), 1.22–1.36 (m, 1H), 1.45–1.63 (m, 2H), 2.00–2.15 (m, 2H), 2.22–2.37 (m, 2H), 2.72–2.99 (m, 5H), 3.12–3.30 (m, 5H), 3.40–3.53 (m, 1H), 3.60–3.77 (m, 1H), 3.90–4.00 (m, 1H), 4.42–4.63 (m, 2H), 5.41–5.55 (m, 1H), 6.90–7.00 (m, 1H), 7.18–7.24 (m, 2H), 7.24–7.35 (m, 2H), 7.45

(dd, $J = 1.8, 10.1$ Hz, 1H). MS: 549 (MH⁺). HRMS (MH⁺) calcd for C₂₈H₃₆Cl₂FN₄O₂, 549.2244; found, 549.2266.

***N*-(1-Aminoethyl)-*N*-[(1*S*)-(2-[4-[(2*R*)-(2-oxo-1-pyrrolidinyl)-3-(2,4-dichlorophenyl)propionyl]-1-piperazinyl]-3-fluorophenyl)-3-methylbutyl]amine Mesylate (10).** A solution of (1*S*)-(2-[4-[(2*R*)-(2-oxo-1-pyrrolidinyl)-3-(2,4-dichlorophenyl)propionyl]-1-piperazinyl]-3-fluorophenyl)-3-methylbutylamine (**9**, 34.0 mg, 0.0615 mmol) in CH₂Cl₂ (1 mL) was treated with glacial acetic acid (7.4 μL) and *tert*-butyl-*N*-(2-oxoethyl)carbamate (14.7 mg, 0.0923 mmol). The mixture was stirred at r.t. for 30 min, and then NaBH(OAc)₃ (26.1 mg, 0.123 mmol) was added. The resulting suspension was stirred at room temperature for 14 h. The reaction mixture was diluted with CH₂Cl₂ (10 mL), transferred to a separatory funnel, and washed with saturated NaHCO₃ aqueous solution (2 × 5 mL). The organic layers were dried over anhydrous MgSO₄, filtered, and concentrated in vacuo. The residue was purified by flash column chromatography on silica gel, eluting with ethyl acetate. The product was obtained as white foam, which was treated with 2 mL of TFA/CH₂Cl₂ (1:1) for 1 h. The excess of TFA and solvent were removed in vacuo, and the crude product was purified by flash column chromatography (5~10% MeOH/CH₂Cl₂) to provide the titled product as a white solid (20 mg, 54%). The free base was converted to the mesylate salt by treatment with 1 equiv of methanesulfonic acid as a white solid; HPLC purity: 99% (220 nm) and 97.8% (254 nm). ¹H NMR (DMSO-*d*₆): 0.86 (d, $J = 6.6$ Hz, 3H), 0.92 (d, $J = 6.6$ Hz, 3H), 1.95 (m, 2H), 2.13 (m, 2H), 2.34 (s, 3H, MeSO₃H), 2.60–3.45 (m, 16H), 3.60 (m, 2H), 4.38 (m, 1H), 4.43 (m, 1H), 5.25 (m, 1H), 5.31 (t, $J = 7.8$ Hz, 1H), 7.30 (brs, 3H), 7.39 (m, 5H), 7.57 (m, 1H). MS: 592 (MH⁺). Anal. (C₃₀H₄₀Cl₂FN₅O₂·MeSO₃H·3H₂O) C, H, N.

***N*-(1*S*)-[2-[4-[(2*R*)-Methyl-3-(4-chlorophenyl)propionyl]-1-piperazinyl]-5-chlorophenyl]-3-methylbutyl)-3-(dimethylamino)propanamide Hydrochloride (12b).** 4-[2-[(1*S*)-((*S*)-*tert*-Butanesulfinylamino)-3-methylbutyl]-4-chlorophenyl]-1-piperazinecarboxylic acid *tert*-butyl ester (**6c**, 21.39 g, 44.1 mmol) was dissolved in CH₂Cl₂ (440 mL) with magnetic stirring. Trifluoroacetic acid (88 mL) was added slowly, and the resulting solution was stirred at r.t. for 1 h. The reaction mixture was slowly poured into 0.5 M K₂CO₃ (500 mL). After all the bubbling had ceased, the mixture was placed in a separatory funnel and the organic layer was separated. The aqueous layer was extracted with CH₂Cl₂ (100 mL), and the combined organics were washed with water and brine, dried over anhydrous MgSO₄, filtered, and concentrated in vacuo to give 4-[2-[(1*S*)-((*S*)-*tert*-butylsulfinylamino)-3-methylbutyl]-4-chlorophenyl]-1-piperazine as a pale yellow foam (18 g), which was used in the next step without further purification.

(2*R*)-methyl-3-(4-chlorophenyl)propionic acid (**16a**, 10.1 g, 50.9 mmol), diisopropylethylamine (17.6 mL, 101 mmol), and HOBt (10.27 g, 76.1 mmol) were sequentially added to a stirring solution of the above compound (16.98 g, 44.1 mmol) in CH₂Cl₂ (220 mL) under N₂. The resulting mixture was stirred at r.t. for 0.5 h. Then EDC (14.58 g, 76.1 mmol) was added portionwise, and the resulting solution was stirred at r.t. overnight. The reaction mixture was placed in a separatory funnel and washed with 0.1 N HCl (200 mL), water, saturated aqueous NaHCO₃, and brine. The organics were dried over MgSO₄, filtered, and concentrated in vacuo. The residue was purified by column chromatography on silica gel, eluting with a 3:1 v/v mixture of hexanes and ethyl acetate, which was gradually increased to a 1:2 ratio, to give *N*-[(1*S*)-[2-[4-[(2*R*)-methyl-3-(2,4-dichlorophenyl)propionyl]-1-piperazinyl]-5-chlorophenyl]-3-methylbutyl)-(*S*)-*tert*-butanesulfinamide (13.80 g, 55% over 2 steps). $R_f = 0.36$ (1:1 v/v hexanes/EtOAc). ¹H NMR (CDCl₃): 0.87 (d, $J = 6.6$ Hz, 3H), 0.92 (d, $J = 6.6$ Hz, 3H), 1.19 (d, $J = 5.7$ Hz, 3H), 1.20 (s, 9H), 1.54–1.39 (m, 2H), 1.75–1.70 (m, 1H), 2.71–2.63 (m, 2H), 2.89–2.82 (m, 1H), 3.01–2.95 (m, 2H), 4.00–3.00 (br, 6H), 4.85 (br, 1H), 6.95 (br, 1H), 7.38–7.13 (m, 7H). MS: 566 (MH⁺).

The above compound (13.78 g, 24.3 mmol) was dissolved in MeOH (243 mL), and HCl (2 M in ether, 15.81 mL, 31.61 mmol) was added. The reaction mixture was stirred at r.t. for 45 min. Nitrogen gas was then bubbled through the reaction mixture to

evaporate residual HCl, and the remaining solvent was removed in vacuo. The residue was dissolved in dichloromethane (250 mL) and washed with saturated NaHCO₃ (3 × 250 mL) and brine (250 mL). The organic layer was separated, dried over anhydrous MgSO₄, filtered, and concentrated in vacuo to give *N*-[(1*S*)-[2-[4-[(2*R*)-methyl-3-(4-chlorophenyl)propionyl]-1-piperazinyl]-5-chlorophenyl]-3-methylbutylamine as an off-white foam in quantitative yield. This compound (11.3 g, 24.32 mmol) was dissolved in dichloromethane (122 mL) along with 3-dimethylaminopropionic acid hydrochloride (3.74 g, 24.32 mmol) and triethylamine (3.42 mL, 24.32 mmol). The reaction mixture was stirred at r.t. for 5 min and then HOBt (3.28 g, 24.3 mmol) was added. After another 5 min, EDC (4.66 g, 24.32 mmol) was added to the reaction mixture, and stirring was continued at r.t. for an additional 8 h. The reaction mixture was washed with saturated NaHCO₃ (3 × 250 mL) and brine (250 mL). The organic layer was dried over anhydrous MgSO₄, filtered, and concentrated in vacuo. The residue was purified by column chromatography on silica using 5% methanol/dichloromethane as the eluent ($R_f = 0.3$) to give the desired product as a free base (10.35 g, 18.42 mmol, 76% yield). HPLC purity: 98.4% (220 nm) and 97.6% (254 nm). ¹H NMR (CDCl₃): 0.93 (d, $J = 6.3$ Hz, 3H), 0.94 (d, $J = 6.3$ Hz, 3H), 1.18 (d, $J = 5.7$ Hz, 3H), 1.22–1.60 (m, 3H), 2.20–2.70 (m, 10H), 2.35 (s, 6H), 2.70–3.62 (m, 5H), 5.44 (m, 1H), 6.89 (d, $J = 8.7$ Hz, 1H), 7.08 (d, $J = 2.4$ Hz, 1H), 7.16 (m, 3H), 7.27 (d, $J = 8.4$ Hz, 2H), 8.94 (d, $J = 8.4$ Hz, 1H). MS: 561 (MH⁺).

N-[(1*S*)-[2-[4-[(2*R*)-Methyl-3-(4-chlorophenyl)propionyl]-1-piperazinyl]-5-chlorophenyl]-3-methylbutyl)-3-(dimethylamino)propanamide (10.02 g, 17.84 mmol) was dissolved in dichloromethane (90 mL). With constant stirring, HCl (2 M in ether, 13.38 mL, 26.76 mmol) was added in one portion. The reaction mixture was stirred at r.t. for 5 min and then nitrogen gas was bubbled through the reaction mixture for 10 min to evaporate excess HCl. The remaining solvent was removed in vacuo. Ether (200 mL) was then added to the solid residue, and the mixture was evaporated to dryness (repeated three times). The residual solid powder was then filtered off and washed with additional ether (3 × 200 mL). The solid was dried in a vacuum oven at 40 °C for 4 h and then at r.t. for 2 days. The product was recovered as a hydrochloride salt in 98% yield (10.49 g, 17.55 mmol) as an off-white powder. $[\alpha]_D^{25} = -22.65$ (1.04, MeOH). ¹H NMR (CDCl₃): 0.86 (d, $J = 5.1$ Hz, 6H), 1.02 (d, $J = 6.6$ Hz, 3H), 1.22 (m, 1H), 1.48 (m, 2H), 2.28 (m, 1H), 2.60 (m, 2H), 2.70 (s, 3H), 2.71 (s, 3H), 2.79 (m, 2H), 3.02 (m, 2H), 3.20 (m, 2H), 3.40 (m, 2H), 4.15 (brs, 4H), 5.33 (m, 1H), 6.97 (d, $J = 8.1$ Hz, 1H), 7.22 (m, 3H), 7.34 (m, 3H), 8.68 (d, $J = 8.1$ Hz, 1H), 10.2 (brs, 1H). MS: 561.3 (MH⁺). Anal. (C₃₀H₄₂Cl₂N₄O₂·HCl·2/3H₂O) C, H, N.

***N*-(1*S*)-[2-[4-[(2*R*)-Methyl-3-(4-chlorophenyl)propionyl]-1-piperazinyl]-5-methylphenyl]-3-methylbutyl)-3-(dimethylamino)propanamide Mesylate (12a).** This compound was synthesized using a procedure similar to that for **12b** from **6b**. HPLC purity: 100% (220 nm) and 95.1% (254 nm). ¹H NMR (DMSO-*d*₆): 0.86 (d, $J = 6.6$ Hz, 6H), 1.04 (d, $J = 6.6$ Hz, 3H), 1.22 (m, 1H), 1.46 (m, 2H), 2.22 (s, 3H), 2.30 (s, 3H, MeSO₃H), 2.40 (m, 1H), 2.56 (m, 4H), 2.60 (s, 6H), 2.80 (m, 1H), 2.80–3.36 (m, 10H), 5.37 (m, 1H), 6.85 (brs, 1H), 6.98 (dd, $J = 1.8, 8.4$ Hz, 1H), 7.08 (d, $J = 1.8$ Hz, 1H), 7.24 (d, $J = 8.1$ Hz, 2H), 7.35 (s, $J = 8.4$ Hz, 2H), 8.44 (d, $J = 8.1$ Hz, 1H). MS: 541 (MH⁺). Anal. (C₃₁H₄₅ClN₄O₂·MeSO₃H·1/2H₂O) C, H, N, S.

***N*-[(1*S*)-1-[2-[4-[(2*R*)-3-(2,4-Dichlorophenyl)-2-(2-oxo-1-pyrrolidinyl)propionyl]-1-piperazinyl]-5-methylphenyl]-3-methylbutyl)-3-(dimethylamino)propanamide Mesylate (13).** This compound was synthesized from **6b** using a procedure similar to that for **9**, followed by a procedure similar to that for **12b**. White solid; HPLC purity: 98.7% (220 nm) and 96.6% (254 nm). ¹H NMR (DMSO-*d*₆): 0.88 (d, $J = 6.6$ Hz, 6H), 1.04 (d, $J = 6.6$ Hz, 3H), 1.27 (m, 1H), 1.46 (m, 2H), 1.91 (m, 1H), 2.09 (m, 1H), 2.23 (s, 3H), 2.28 (s, 3H, MeSO₃H), 2.35–2.60 (m, 9H), 2.63 (s, 6H), 2.80 (m, 1H), 2.88–3.50 (m, 6H), 5.37 (m, 1H), 6.86 (brs, 1H), 6.98 (dd, $J = 1.8, 8.4$ Hz, 1H), 7.08 (d, $J = 1.8$ Hz, 1H), 7.24 (d, $J =$

8.1 Hz, 2H), 7.35 (d, $J = 8.4$ Hz, 2H), 8.44 (d, $J = 8.1$ Hz, 1H). MS: 644 (MH⁺). Anal. (C₃₄H₄₇Cl₂N₅O₃·MeSO₃H) C, H, N, S.

4S-Benzyl-3-[3-(4-chlorophenyl)-2R-methylpropionyl]oxazolidin-2-one (15a). (*S*)-4-benzyl-3-propionyloxazolidin-2-one (**14**, 46.7 g, 200 mmol) was dissolved in THF (870 mL) under an inert atmosphere (N₂). This was then cooled to -70 °C (dry ice/acetone) and treated with sodium hexamethyldisilazide (110 mL of a 2.0 M solution in THF, 220 mmol) in a dropwise fashion (addition lasted for ~45 min). The resulting mixture was stirred at -70 °C for 1 h. A solution of 4-chlorobenzyl bromide (53.4 g, 260 mmol) in THF (160 mL) was then added dropwise over 30 min. The resulting mixture was stirred at -70 °C for 6 h and then allowed to warm to r.t. overnight. The reaction was carefully quenched with water (100 mL), and the solvent was removed in vacuo. The resulting slurry was suspended in water (200 mL) and filtered. The solid was rinsed with EtOAc and air-dried to give the desired product (36.67 g, 102.6 mmol, 51%). A second crop of product was obtained from the filtrates after the organic layer was separated, washed with brine, dried over MgSO₄, and concentrated in vacuo. The resulting brown solid was suspended in MeOH and filtered to give 17.22 g (48.2 mmol, 24%) of the desired product. Total yield, 53.89 g (75%). Only one diastereomer was observed by ¹H NMR, and stereochemistry was confirmed by single crystal X-ray analysis. ¹H NMR (CDCl₃): 1.18 (d, $J = 6.3$ Hz, 3H), 2.66–2.56 (m, 2H), 3.16–3.07 (m, 2H), 4.22–4.02 (m, 3H), 4.71–4.63 (m, 1H), 7.08–7.05 (m, 2H), 7.32–7.21 (m, 7H).

2R-Methyl-3-(4-chlorophenyl)propionic Acid (16a). 4S-Benzyl-3-[3-(4-chlorophenyl)-2R-methylpropionyl]oxazolidin-2-one (**15a**, 53.89 g, 150.7 mmol) was dissolved in a 4:1 v/v THF/H₂O mixture (750 mL) and cooled to 0 °C (ice/water bath). Hydrogen peroxide 50% (60 mL) was added slowly, followed by a solution of lithium hydroxide monohydrate (11.08 g, 263.7 mmol) in H₂O (380 mL). The resulting mixture was stirred at 0 °C for 1.5 h. Na₂SO₃·7H₂O (155.70 g, 618.0 mmol) dissolved in H₂O (250 mL) was added at 0 °C, and the resulting mixture was allowed to slowly reach r.t. The volatiles were removed in vacuo, and the aqueous residue was extracted with CH₂Cl₂ (2 × 300 mL). The aqueous layer was separated, made acidic with 2.0 N HCl, and then extracted with EtOAc (2 × 250 mL). The organics were washed with brine, dried over MgSO₄, and concentrated in vacuo to give the titled compound as an oil that solidified upon standing (29.80 g, 150.1 mmol, 99%). ¹H NMR (CDCl₃): 1.18 (d, $J = 6.3$ Hz, 3H), 2.80–2.62 (m, 2H), 3.02 (dd, $J = 6.0, 12.6$ Hz, 1H), 7.12 (d, $J = 8.7$ Hz, 2H), 7.26 (d, $J = 8.7$ Hz, 2H). [α]_D²⁵ = -27.930 (c 8.685 mg/cc, MeOH).⁴⁰

4-[3-[(1R)-((S)-tert-Butanesulfinylamino)-3-methylbutyl]-2-pyridinyl]-1-piperazinecarboxylic Acid tert-Butyl Ester (R-19a). Lithium diisopropylamide (131 mL, 262 mmol, 2 M in THF) was added to a stirring solution of 2-bromopyridine (25 mL, 262 mmol) in THF (208 mL) at -78 °C under nitrogen. The reaction mixture was stirred at -78 °C for 2 h and then a solution of DMF (20.3 mL, 262 mmol) in THF (104 mL) was added. After the addition, the reaction mixture was allowed to warm to r.t. and was neutralized by adding to a saturated solution of ammonium chloride. The crude product was extracted with ethyl acetate (3 × 200 mL), the organic layers were combined, dried over anhydrous Na₂SO₄, and filtered, and solvent was removed in vacuo. The residue was purified by column chromatography on silica using 15% ethyl acetate/hexanes as the eluent ($R_f = 0.3$). The product 2-bromo-3-formylpyridine **17a** was obtained as yellow oil (9.4 g, 50.5 mmol, 19% yield).

2-Bromo-3-formylpyridine (**17a**, 9.4 g, 50.5 mmol) was dissolved in DMF (100 mL) along with diisopropylethylamine (8.8 mL, 50.5 mmol) and 1-Boc-piperazine (9.4 g, 50.5 mmol) in a reaction flask. The reaction mixture was heated at 100 °C for 8 h, then cooled to r.t., and quenched with saturated NaHCO₃ (150 mL). The product was extracted with ethyl acetate (3 × 100 mL), the organic layers were combined, dried over anhydrous Na₂SO₄, and filtered, and the solvent was removed in vacuo. The residue was purified by column chromatography on silica using 25% ethyl acetate/hexanes

as the eluent ($R_f = 0.3$). The product 2-(4-Boc-1-piperazinyl)-3-formylpyridine was obtained as a yellow solid (9.8 g, 33.5 mmol, 67% yield).

2-(4-Boc-1-piperazinyl)-3-formylpyridine (3 g, 10.3 mmol) was dissolved in THF (51 mL) along with (*S*)-tert-butanesulfinamide (1.4 g, 11.3 mmol) and titanium(IV) ethoxide (8.6 mL, 41.2 mmol). The reaction mixture was allowed to stir at r.t. for 8 h and then brine (20 mL) was added. The reaction mixture was filtered, and the solid was washed with ethyl acetate (3 × 75 mL). The organic layer was collected, dried over anhydrous Na₂SO₄, filtered, and concentrated in vacuo to give the titled compound as a yellow solid in quantitative yield without further purification (4.1 g, 10.3 mmol).

The above intermediate (4.1 g, 10.3 mmol) in THF (30 mL) was cooled to -40 °C, and Me₃Al (15.45 mL, 30.9 mmol) was added. The reaction mixture was allowed to stir at -40 °C under nitrogen atmosphere for 20 min and was then cooled to -78 °C. To the reaction mixture, isobutyl lithium (12.9 mL, 20.6 mmol, 1.6 M in heptane) was added slowly. After the addition was complete, the reaction was warmed to r.t. and carefully quenched with water. The mixture was then concentrated in vacuo and diluted with dichloromethane (150 mL). The organic layer was then washed with saturated NaHCO₃ solution (2 × 100 mL) and brine (100 mL), dried over anhydrous MgSO₄, filtered, and concentrated in vacuo. The residue was purified by column chromatography on silica using 75% ethyl acetate/hexanes as the eluent ($R_f = 0.3$). The titled product was obtained as a yellow solid (2.8 g, 6.15 mmol, 60%). ¹H NMR (CDCl₃): 0.89 (d, $J = 6.3$ Hz, 3H), 0.94 (d, $J = 6.0$ Hz, 3H), 1.21 (s, 9H), 1.47 (s, 9H), 1.24–1.30 (m, 2H), 1.5–1.58 (m, 1H), 2.80–3.40 (m, 4H), 3.40–3.70 (m, 4H), 4.69 (dd, $J = 6.9$ Hz, 1H), 7.06 (dd, $J = 4.8$ Hz, 1H), 7.61 (dd, $J = 1.8$ Hz, 1H), 8.29 (dd, $J = 1.8$ Hz, 1H).

4-[3-[(1R)-((S)-tert-Butanesulfinylamino)-3-methylbutyl]-6-methyl-2-pyridinyl]-1-piperazinecarboxylic Acid tert-Butyl Ester (R-19b). This compound was synthesized from 2-bromo-6-methylpyridine and *S*-tert-butanesulfinamide using a procedure similar to that for **19a**. ¹H NMR (CDCl₃): 0.87 (d, $J = 6.0$ Hz, 3H), 0.94 (d, $J = 6.0$ Hz, 3H), 1.12 (s, 9H), 1.46 (s, 9H), 1.48–1.58 (m, 2H), 1.70–1.78 (m, 1H), 2.43 (s, 3H), 2.8–3.05 (m, 4H), 3.40–3.78 (m, 4H), 4.64 (dd, $J = 6.9$ Hz, 1H), 6.89 (d, $J = 7.8$ Hz, 1H), 7.46 (d, $J = 7.8$ Hz, 1H). A small sample was crystallized in ether/hexanes to give single crystals for X-ray determination.

1-[3-[(1R)-Amino-3-methylbutyl]-2-pyridinyl]-4-[3-(2,4-dichlorophenyl)propionyl]piperazine Trifluoroacetate (R-20a). 4-[3-[(1R)-((S)-tert-Butanesulfinylamino)-3-methylbutyl]-2-pyridinyl]-1-piperazinecarboxylic acid tert-butyl ester (**R-19a**, 452.6 mg, 1 mmol) was allowed to stir at r.t. for 1.5 h in a 20% TFA/CH₂Cl₂ mixture (20 mL). The reaction was quenched with saturated NaHCO₃ solution (5 mL). The organic layer was washed with saturated NaHCO₃ solution (2 × 10 mL) and brine (10 mL), dried over anhydrous MgSO₄, filtered, and concentrated in vacuo. The deprotected intermediate was recovered in quantitative yield. A small portion of this piperazine intermediate (35.2 mg, 0.1 mmol) was dissolved in dichloromethane (0.5 mL) along with HOBt (13.5 mg, 0.1 mmol), NaHCO₃ (8.4 mg, 0.1 mmol), and 3-(2,4-dichlorophenyl)propanoic acid (21.9 mg, 0.1 mmol). The reaction mixture was allowed to stir at r.t. for 10 min and then EDC (19.2 mg, 0.1 mmol) was added. The reaction was then stirred for an additional 8 h followed by quenching with saturated NaHCO₃ solution. The organic layer was separated, washed with brine (2 mL), dried over anhydrous MgSO₄, filtered, and concentrated in vacuo. The resulting residue was dissolved in MeOH (2 mL), and 0.2 M HCl/ether (1 mL) was added. The reaction was stirred at r.t. for 1 h and then solvent was removed under a stream of nitrogen. The crude product was purified by prep HPLC to yield the desired product as the TFA salt (15 mg, 0.026 mmol, 26% yield). Light yellow foam; HPLC purity: 98% (220 nm) and 95% (254 nm). ¹H NMR (CD₃OD): 0.95 (d, $J = 6.6$ Hz, 3H), 1.03 (d, $J = 6.6$ Hz, 3H), 1.37–1.53 (m, 1H), 1.69–1.82 (m, 1H), 1.82–1.93 (m, 1H), 2.76 (t, $J = 7.7$ Hz, 2H), 2.85–2.96 (m, 4H), 3.00–3.13 (m, 4H), 3.55–3.64 (m, 1H), 3.64–3.84 (m, 3H), 4.83 (t, $J = 7.5$ Hz, 1H), 7.24–7.38 (m, 3H), 7.44 (d, $J = 4.1$ Hz, 1H), 7.90 (dd, $J = 1.8,$

7.7 Hz, 1H), 8.39 (dd, $J = 1.8, 4.8$ Hz, 1H). MS: 449 (MH⁺). HRMS (MH⁺) calcd for C₂₃H₃₁Cl₂N₄O, 449.1875; found, 449.1892.

1-[3-[(1S)-Amino-3-methylbutyl]-2-pyridinyl]-4-[3-(2,4-dichlorophenyl)propionyl]piperazine Trifluoroacetate (S-20a). This compound was synthesized using the same method for *R*-20a from *S*-tert-butanesulfonamide. Light yellow foam, HPLC purity: 92% (220 nm) and 96% (254 nm). ¹H NMR (CD₃OD): 0.95 (d, $J = 6.6$ Hz, 3H), 1.03 (d, $J = 6.6$ Hz, 3H), 1.37–1.53 (m, 1H), 1.69–1.82 (m, 1H), 1.82–1.93 (m, 1H), 2.76 (t, $J = 7.7$ Hz, 2H), 2.85–2.96 (m, 4H), 3.00–3.13 (m, 4H), 3.55–3.64 (m, 1H), 3.64–3.84 (m, 3H), 4.83 (t, $J = 7.5$ Hz, 1H), 4.83 (t, $J = 7.5$ Hz, 1H), 7.24–7.38 (m, 3H), 7.44 (d, $J = 4.1$ Hz, 1H), 7.90 (dd, $J = 1.8, 7.7$ Hz, 1H), 8.39 (dd, $J = 1.8, 4.8$ Hz, 1H). MS: 449 (MH⁺).

1-[3-[(1R)-1-Amino-3-methylbutyl]-2-pyridinyl]-4-[2-methyl-3-(2,4-dichlorophenyl)propionyl]piperazine Trifluoroacetate (R-20b). This compound was synthesized from *R*-19a and 2-methyl-3-(2,4-dichlorophenyl)propionic acid using a procedure similar to that for *R*-20a. Light yellow foam; HPLC purity: 97% (220 and 254 nm). ¹H NMR (CD₃OD): 0.94 (d, $J = 6.6$ Hz, 3H), 1.01 (d, $J = 6.6$ Hz, 3H), 1.19 and 1.20 (d, $J = 6.6$ Hz, 3H), 1.34–1.50 (m, 1H), 1.67–1.91 (m, 2H), 2.40–2.54 (m, 1H), 2.60–2.76 (m, 1H), 2.80–3.08 (m, 5H), 3.32–3.46 (m, 2H), 3.52–3.88 (m, 4H), 4.81 (t, $J = 7.5$ Hz, 1H), 7.24–7.30 (m, 3H), 7.42–7.47 (m, 1H), 7.83–7.89 (m, 1H), 8.39 (dd, $J = 1.8, 4.8$ Hz, 1H). MS: 463 (MH⁺).

1-[3-[(1R)-1-Amino-3-methylbutyl]-6-methyl-2-pyridinyl]-4-[2R-methyl-3-(2,4-dichlorophenyl)propionyl]piperazine Trifluoroacetate (R-21). This compound was synthesized from *R*-19b and 2R-methyl-3-(2,4-dichlorophenyl)propionic acid using a procedure similar to that for *R*-20a. Light yellow foam; HPLC purity: 100% (220 and 254 nm). ¹H NMR (CD₃OD): 0.92 (d, $J = 6.6$ Hz, 3H), 1.00 (d, $J = 6.6$ Hz, 3H), 1.21 (d, $J = 6.6$ Hz, 3H), 1.32–1.47 (m, 1H), 1.65–1.88 (m, 2H), 2.39–2.50 (m, 1H), 2.47 (s, 3H), 2.78–3.04 (m, 6H), 3.32–3.45 (m, 2H), 3.54–3.80 (m, 4H), 4.75 (t, $J = 7.5$ Hz, 1H), 7.12 (d, $J = 7.9$ Hz, 1H), 7.24–7.28 (m, 2H), 7.43 (d, $J = 1.3$ Hz, 1H), 7.71 (d, $J = 7.9$ Hz, 1H). MS: 477 (MH⁺). HRMS (MH⁺) calcd for C₂₅H₃₄Cl₂N₄O, 477.2188; found, 477.2165.

***N*-((1R)-[2-[4-[2R-Methyl-3-(2,4-dichlorophenyl)propionyl]-1-piperazinyl]-3-pyridinyl]-3-methylbutyl)-2-aminoacetamide Mesylate Trifluoroacetate (R-22).** This compound was synthesized from *R*-20b using a procedure similar to that for **11**. White solid; HPLC purity: 99% (220 nm) and 98% (254 nm). ¹H NMR (CD₃OD): 0.94 (d, $J = 6.1$ Hz, 3H), 0.96 (d, $J = 6.1$ Hz, 3H), 1.18 and 1.20 (d, $J = 6.6$ Hz, 3H), 1.34–1.50 (m, 1H), 1.50–1.66 (m, 2H), 2.42–2.54 (m, 1H), 2.60–2.70 (m, 1H), 2.74–3.14 (m, 5H), 3.20–3.42 (m, 2H), 3.52–3.86 (m, 7H), 5.36–5.45 (m, 1H), 7.12–7.19 (m, 1H), 7.23–7.26 (m, 2H), 7.42 and 7.46 (d, $J = 1.8$ Hz, 1H), 7.72–7.78 (m, 1H), 8.17–8.22 (m, 1H). MS: 520 (MH⁺). HRMS (MH⁺) calcd for C₂₆H₃₆Cl₂N₅O₂, 520.2246; found, 520.2236.

***N*-((1S)-[2-[4-[2R-Methyl-3-(2,4-dichlorophenyl)propionyl]-1-piperazinyl]-3-pyridinyl]-3-methylbutyl)-2-aminoacetamide Trifluoroacetate (S-22).** This compound was synthesized from *S*-20 using a procedure similar to that for **11**. Light yellow foam; HPLC purity: 100% (220 and 254 nm). ¹H NMR (CD₃OD): 0.94 (d, $J = 6.1$ Hz, 3H), 0.96 (d, $J = 6.1$ Hz, 3H), 1.18 and 1.20 (d, $J = 6.6$ Hz, 3H), 1.34–1.50 (m, 1H), 1.50–1.66 (m, 2H), 2.42–2.54 (m, 1H), 2.60–2.70 (m, 1H), 2.74–3.14 (m, 5H), 3.20–3.42 (m, 2H), 3.52–3.86 (m, 7H), 5.36–5.45 (m, 1H), 7.12–7.19 (m, 1H), 7.23–7.26 (m, 2H), 7.42 and 7.46 (d, $J = 1.8$ Hz, 1H), 7.72–7.78 (m, 1H), 8.17–8.22 (m, 1H). MS: 520 (MH⁺). HRMS (MH⁺) calcd for C₂₆H₃₆Cl₂N₅O₂, 520.2246; found, 520.2236.

***N*-((1R)-[2-[4-[2R-Methyl-3-(2,4-dichlorophenyl)propionyl]-1-piperazinyl]-6-methyl-3-pyridinyl]-3-methylbutyl)-3-(dimethylamino)propionamide (R-23).** This compound was synthesized from *R*-21 using a procedure similar to that for **12b**. White solid; HPLC purity: 96.1% (220 nm) and 96.5% (254 nm). ¹H NMR (CDCl₃): 0.91 (d, $J = 6.5$ Hz, 3H), 0.93 (d, $J = 6.5$ Hz, 3H), 1.17 (d, $J = 7.0$ Hz, 3H), 1.40 (m, 1H), 1.47 (m, 2H), 2.37 (s, 6H), 2.42 (s, 3H), 2.43 (m, 2H), 2.52 (m, 1H), 2.67 (m, 2H), 2.83 (m, 2H), 3.03 (dd, $J = 8.0, 13.0$ Hz, 1H), 3.18 (dd, $J = 7.0, 14.5$ Hz, 1H), 3.22 (m, 1H), 3.35 (m, 1H), 3.42 (m, 1H), 3.58 (m, 2H), 3.88 (m, 1H), 5.28 (m, 1H), 6.83 (d, $J = 7.5$ Hz, 1H), 7.17 (dd, $J = 2.0, 8.5$

Hz, 1H), 7.19 (d, $J = 8.5$ Hz, 1H), 7.33 (m, 2H), 8.60 (brs, 1H). MS: 576 (MH⁺). Anal. (C₃₀H₄₃Cl₂N₃O₂·H₂O) C, H, N.

Supporting Information Available: Synthetic procedure for the preparation of compound **6c**, analytic data of key compounds, and description of pharmacokinetic studies and protocol for the murine cachexia model. This material is available free of charge via the Internet at <http://pubs.acs.org>.

References

- Gordon, J. N.; Green, S. R.; Goggin, P. M. Cancer cachexia. *QJM* **2005**, *98*, 779–788.
- Bossola, M.; Pacelli, F.; Tortorelli, A.; Doglietto, G. B. Cancer cachexia: it's time for more clinical trials. *Ann. Surg. Oncol.* **2007**, *14*, 276–285.
- Osei-Hyiaman, D. Endocannabinoid system in cancer cachexia. *Curr. Opin. Clin. Nutr. Metab. Care* **2007**, *10*, 443–448.
- Akamizu, T.; Kangawa, K. Emerging results of anticatabolic therapy with ghrelin. *Curr. Opin. Clin. Nutr. Metab. Care* **2007**, *10*, 278–283.
- DeBoer, M. D. Melanocortin interventions in cachexia: how soon from bench to bedside. *Curr. Opin. Clin. Nutr. Metab. Care* **2007**, *10*, 457–462.
- Ballesteros, J. A.; Shi, L.; Javitch, J. A. Structural mimicry in G-protein-coupled receptors: Implications of the high-resolution structure of rhodopsin for structure-function analysis of rhodopsin-like receptors. *Mol. Pharmacol.* **2001**, *60*, 1–19.
- Goodfellow, V. S.; Saunders, J. The melanocortin system and its role in obesity and cachexia. *Curr. Top. Med. Chem.* **2003**, *3*, 855–883.
- Wilczynski, A. M.; Joseph, C. G.; Haskell-Luevano, C. Current trends in the structure–activity relationship studies of the endogenous agouti-related protein (AGRP) melanocortin receptor antagonist. *Med. Res. Rev.* **2005**, *25*, 545–556.
- Cone, R. D. The central melanocortin system and energy homeostasis. *Trends Endocrinol. Metab.* **1999**, *10*, 211–216.
- Tao, Y. X.; Segaloff, D. L. Functional analyses of melanocortin-4 receptor mutations identified from patients with binge eating disorder and nonobese or obese subjects. *J. Clin. Endocrinol. Metab.* **2005**, *90*, 5632–5638.
- MacKenzie, R. G. Obesity-associated mutations in the human melanocortin-4 receptor gene. *Peptides* **2006**, *27*, 395–403.
- Boyce, R. S.; Duhl, D. M. Melanocortin-4 receptor agonists for the treatment of obesity. *Curr. Opin. Investig. Drugs* **2004**, *5*, 1063–1071.
- Foster, A. C.; Joppa, M.; Markison, S.; Gogas, K. R.; Fleck, B. A. Body weight regulation by selective MC4 receptor agonists and antagonists. *Ann. N.Y. Acad. Sci.* **2003**, *994*, 103–110.
- DeBoer, M. D.; Marks, D. L. Therapy insight: Use of melanocortin antagonists in the treatment of cachexia in chronic disease. *Nat. Clin. Pract. Endocrinol. Metab.* **2006**, *2*, 459–466.
- Li, S. J.; Varga, K.; Archer, P.; Hruby, V. J.; Sharma, S. D. Melanocortin antagonists define two distinct pathways of cardiovascular control by alpha- and gamma-melanocyte-stimulating hormones. *J. Neurosci.* **1996**, *16*, 5182–5188.
- Wisse, B. E.; Frayo, R. S.; Schwartz, M. W.; Cummings, D. E. Reversal of cancer anorexia by blockade of central melanocortin receptors in rats. *Endocrinology* **2001**, *142*, 3292–3301.
- Marks, D. L.; Butler, A. A.; Turner, R.; Brookhart, G.; Cone, R. D. Differential role of melanocortin receptor subtypes in cachexia. *Endocrinology* **2003**, *144*, 1513–1523.
- Joppa, M. A.; Gogas, K. R.; Foster, A. C.; Markison, S. Central infusion of the melanocortin receptor antagonist agouti-related peptide (AgRP(83–132)) prevents cachexia-related symptoms induced by radiation and colon-26 tumors in mice. *Peptides* **2007**, *28*, 636–642.
- Foster, A. C.; Chen, C. Melanocortin-4 receptor antagonists as potential therapeutics in the treatment of cachexia. *Curr. Top. Med. Chem.* **2007**, *7*, 1131–1136.
- Marks, D. L.; Cone, R. D. The role of the melanocortin-3 receptor in cachexia. *Ann. N.Y. Acad. Sci.* **2003**, *994*, 258–266.
- Vos, T. J.; Caracoti, A.; Che, J. L.; Dai, M.; Farrer, C. A. Identification of 2-[2-[2-(5-bromo-2-methoxyphenyl)-ethyl]-3-fluorophenyl]-4,5-dihydro-1H-imidazole (ML00253764), a small molecule melanocortin 4 receptor antagonist that effectively reduces tumor-induced weight loss in a mouse model. *J. Med. Chem.* **2004**, *47*, 1602–1604.
- Nicholson, J. R.; Kohler, G.; Schaerer, F.; Senn, C.; Weyeremann, P. Peripheral administration of a melanocortin 4-receptor inverse agonist prevents loss of lean body mass in tumor-bearing mice. *J. Pharmacol. Exp. Ther.* **2006**, *317*, 771–777.
- Tucci, F. C.; White, N. S.; Markison, S.; Joppa, M.; Tran, J. A. Potent and orally active nonpeptide antagonists of the human melanocortin-4 receptor based on a series of trans-2-disubstituted

- cyclohexylpiperazines. *Bioorg. Med. Chem. Lett.* **2005**, *15*, 4389–4395.
- (24) Markison, S.; Foster, A. C.; Chen, C.; Brookhart, G. B.; Hesse, A. The regulation of feeding and metabolic rate and the prevention of murine cancer cachexia with a small-molecule melanocortin-4 receptor antagonist. *Endocrinology* **2005**, *146*, 2766–2773.
- (25) Foster, A. C.; Chen, C.; Markison, S.; Marks, D. L. MC4 receptor antagonists: A potential treatment for cachexia. *IDrugs* **2005**, *8*, 314–319.
- (26) Nozawa, D.; Okubo, T.; Ishii, T.; Kakinuma, H.; Chaki, S. Structure–activity relationships of novel piperazines as antagonists for the melanocortin-4 receptor. *Bioorg. Med. Chem.* **2007**, *15*, 1989–2005.
- (27) Nozawa, D.; Okubo, T.; Ishii, T.; Takamori, K.; Chaki, S. Novel piperazines: Potent melanocortin-4 receptor antagonists with anxiolytic-like activity. *Bioorg. Med. Chem.* **2007**, *15*, 2375–2385.
- (28) Vos, T. J.; Balani, S.; Blackburn, C.; Chau, R. W.; Danca, M. D. Identification and structure–activity relationships of a new series of melanocortin-4 receptor antagonists. *Bioorg. Med. Chem. Lett.* **2006**, *16*, 2302–2305.
- (29) Poitout, L.; Brault, V.; Sackur, C.; Bernetiere, S.; Camara, J.; et al. Identification of a novel series of benzimidazoles as potent and selective antagonists of the human melanocortin-4 receptor. *Bioorg. Med. Chem. Lett.* **2007**.
- (30) Chen, C. W.; Tran, J. A.; Jiang, W.; Tucci, F. C.; Arellano, M. Propionylpiperazines as human melanocortin-4 receptor ligands. *Bioorg. Med. Chem. Lett.* **2006**, *16*, 4800–4803.
- (31) Jiang, W.; Chen, C.; Marinkovic, D.; Tran, J. A.; Chen, C. W. Practical asymmetric synthesis of alpha-branched 2-piperazinylbenzylamines by 1,2-additions of organometallic reagents to *N-tert*-butanesulfinyl imines. *J. Org. Chem.* **2005**, *70*, 8924–8931.
- (32) Jiang, W.; Tucci, F. C.; Chen, C. W.; Arellano, M.; Tran, J. A. Arylpropionylpiperazines as antagonists of the human melanocortin-4 receptor. *Bioorg. Med. Chem. Lett.* **2006**, *16*, 4674–4678.
- (33) Tran, J. A.; Tucci, F. C.; Jiang, W.; Marinkovic, D.; Chen, C. W. Pyrrolidinones as orally bioavailable antagonists of the human melanocortin-4 receptor with anti-cachectic activity. *Bioorg. Med. Chem.* **2007**, *15*, 5166–5176.
- (34) Kotake, T.; Hayashi, Y.; Rajesh, S.; Mukai, Y.; Takiguchi, Y. Design and synthesis of a new polymer-supported Evans-type oxazolidinone: An efficient chiral auxiliary in the solid-phase asymmetric alkylation reactions. *Tetrahedron* **2005**, *61*, 3819–3844.
- (35) Numata, A.; Kondo, Y.; Sakamoto, T. General synthetic method for naphthyridines and their N-oxides containing isoquinolinic nitrogen. *Synthesis* **1999**, *306*, 311.
- (36) Nickolls, S. A.; Cismowski, M. I.; Wang, X.; Wolff, M.; Conlon, P. J. Molecular determinants of melanocortin 4 receptor ligand binding and MC4/MC3 receptor selectivity. *J. Pharmacol. Exp. Ther.* **2003**, *304*, 1217–1227.
- (37) Loscher, W.; Potschka, H. Blood–brain barrier active efflux transporters: ATP-binding cassette gene family. *NeuroRx* **2005**, *2*, 86–98.
- (38) Jiang, J.; Tucci, F. C.; Tran, J. A.; Fleck, B. A.; Wen, J. et al. Pyrrolidinones as potent functional antagonists of the human melanocortin-4 receptor. *Bioorg. Med. Chem. Lett.* **2007**, *17*, 5610–5613.
- (39) Konturek, S. J.; Konturek, J. W.; Pawlik, T.; Brzozowski, T. Brain–gut axis and its role in the control of food intake. *J. Physiol. Pharmacol.* **2004**, *55*, 137–154.
- (40) Ferorelli, S.; Loiodice, F.; Tortorella, V.; Amoroso, R.; Bettoni, G. Isosteres of chiral clofibrac acid analogs: synthesis, resolution, absolute configuration and HPLC detection of the optical purity. *Farmaco* **1999**, *52*, 367–374.

JM701137S